Long-Term Double Integration of Acceleration for Position Sensing and Frequency Domain System Identification

Hunter B. Gilbert, Ozkan Celik, *Student Member, IEEE,* Marcia K. O'Malley, *Member, IEEE*

Abstract— We present results from successful implementation of long-term ($>$10 seconds) real-time integration of acceleration to measure position. We evaluated two analog circuit designs for double integration of an acceleration signal. Our circuit design features three high-pass filters and two first order integrators, leading to a critically damped double integrator. The second design we have implemented is a second order underdamped integrator reported in the literature. Accuracy of both circuits in sensing position based on only accelerometer readings was experimentally evaluated by comparison with encoder readings. We conclude that a critically damped double integrator coupled with an accelerometer is well-suited for frequency domain system identification, thanks to reliable position measurement capability with minimal interference to system dynamics.

Index Terms— Accelerometers, long-term integration of acceleration, frequency domain system identification, double integrator

I. INTRODUCTION

In this study, we present experimental results on accuracy of position measurements obtained by long-term double integration of acceleration in analog circuitry. We evaluate and compare two different analog circuitry designs: a single-stage underdamped double integrator circuit reported in the literature and a two-stage critically damped double integrator circuit we have developed.

Using accelerometers and integrating the acceleration to obtain position instead of using position sensors poses several advantages such as avoiding tight tolerances for alignment in sensor installation, reducing cost, and causing minimal interference to original system dynamics. Although double integration of acceleration can seem trivial in theory, implementation involves significant challenges. These challenges include need for noise-free signals especially in the low frequency range, extreme sensitivity to DC offsets that lead to significant drifts and saturation during integration, and loss of information during discretization and quantization.

Nevertheless, there have been attempts reported in the literature to overcome these challenges. Some novel attempts use knowledge of the kinematics of multi-degree-of-freedom systems to compute joint angles [1], but long-term integration of accelerometer signals to achieve velocity and position signals has been largely unsuccessful due to integration of small DC offsets resulting in linear and quadratic errors in velocity and position, respectively [2]. This problem has been addressed for sensing position using dead-reckoning

H. B. Gilbert, O. Celik and M. K. O'Malley are with the Department of Mechanical Engineering and Materials Science, Rice University, Houston, TX 77005 (e-mails: hbg1@rice.edu, celiko@rice.edu, omalleym@rice.edu)

by the use of resetting, where integration is carried out only for a very short period of time and the position is repeatedly corrected by an external source such as a GPS or a rate gyroscope [3]. Thong, et. al. [2] have developed RMS error estimates for numerical double integration of noisy accelerometer signals. Ball and Lewis [4] reported an analysis of error due to noise in analog circuits. Short-term integration can be successful; for example, Croker determined the position of an engine valve during one opening and closing cycle [5]. Similarly, Balasubramaniam et al. [6] obtained position out of 40 ms-long acceleration recordings to be used in system identification.

In contrast, long-term integration is more challenging due to the issues of drift and sensitivity to DC offsets and noise. Despite these challenges, long-term integration has been shown to be achievable under certain circumstances. These conditions include carrying out the integration in continuous domain to avoid problems posed by quantization and discretization, and existence of a lower-bound in the frequency domain for the signal that is to be integrated to avoid drift and saturation. The requirement for a lower-bound in the frequency domain limits the application of long-term acceleration integration to sensing velocity or position of mechanical vibrations. An example of analog single integration of an acceleration signal was given in a vehicle vibration measurement application in [7]. Viswanathan and Baghialakshmi [8] provided a practical implementation of a single-stage underdamped double integrator in the continuous domain using operational amplifiers (op-amps). They reported an overall accuracy of $\pm$5% for displacement recordings based on double integrated acceleration; however, this evaluation was based on only peak displacement measurements and the details of the position sensing system used for validation was not reported. In our study, we replicated the integrator design of Viswanathan and Baghialakshmi with only slight modifications to improve its performance and we evaluated its position sensing accuracy. In a similar study, Lewis and Ball [9] reported use of a long-term double integrator used to successfully measure velocity and position of structural vibrations. Since Lewis and Ball did not provide their circuit design, we were not able to conduct an evaluation of the accuracy and performance of their double integrator design.

In this paper, we present a two-stage critically damped integrator design that allows accurate long-term real-time single and double integration of accelerometer signals to provide velocity and position sensing. In our study, we have evaluated position sensing performance and accuracy of our integrator design as well as Viswanathan and Baghialak-

shmi's integrator design [8] by comparing their position output with high resolution (1 μm) optical encoder readings. We show that accurate long-term real-time single and double integration of accelerometer signals is possible with a critically damped integrator design while the underdamped design suffers from a need for extremely long settling periods in the order of seconds which renders them impractical. One application area for our double integrator design is frequency domain system identification of mechanical systems. With our double integrator implementation, force-input, position-output models can be obtained effectively without altering the dynamics of the system, since the only sensing element to be attached on the system would be an accelerometer with a mass of only several grams.

The paper is structured as follows: Section II presents the details of the experimental setup and the analog circuit designs. Verification of experimental implementation of designed analog circuits and accuracy of position signals are presented and discussed in Section III. The paper concludes with a discussion of implications, contributions and limitations of the study.

II. METHODS

A. Experimental Setup

The essential components of the experimental setup are the accelerometer and the linear encoder used as a reliable reference position source, and the choice of these components was based on the mechanical system which they will be used to measure. A 4-inch speaker with 8Ω nominal impedance provides a good platform for testing double integration of acceleration for vibrating motion, because it has a relatively low resonant frequency and responds to a wide range of amplitudes and frequencies. We used a Logosol pulse width modulated DC servo amplifier to drive the speaker.

For a sinusoidal input of $A\sin(2\pi f t)$, the maximum acceleration of the speaker cone is given by $4A\pi^2 f^2$, where A is the amplitude of vibration and f is the frequency in Hz. For a 20 Hz signal at 1 mm of travel, this corresponds to a peak acceleration of about 15.8 m/s^2, or 1.6g. An Entran EGA-F-25 single-axis accelerometer with a sensitivity of 4.045 mV/g and a full scale range of 25g was used to capture the vibration of the speaker in the frequency range of 10 to 100 Hz, providing high resolution and avoiding saturation.

The linear encoder used is a Renishaw RGH24X. The speaker cone has a rod glued to it which is affixed to a linear slide as depicted in Fig. 1. The encoder read head is mounted to the movable element of the slide and reads relative to the fixed base. The RGH24X has a resolution of 1 μm. The absolute quantization error is thus 0.5 μm, so for a speaker displacement of 1 mm, the relative error is 0.05%. This accuracy is more than sufficient for the linear encoder to perform as a reference for evaluation of the accelerometer-based position signal.

We present the results from two separate analog double integration circuits. All of the filters are implemented with LF412 operational amplifiers (op-amps) with the exception of the input amplifier that is connected to the accelerometer.
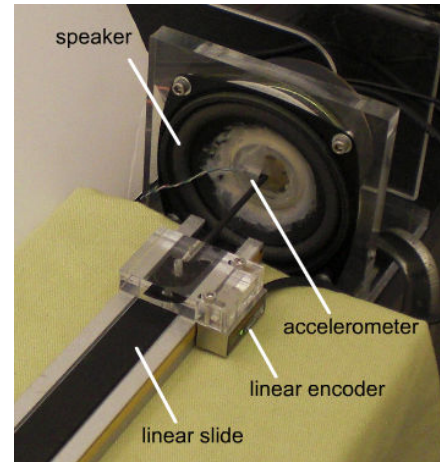
Fig. 1. Experimental setup: an accelerometer and a linear encoder attached to a speaker.

An Analog Devices AD620 instrumentation amplifier is used for this purpose because of its low offset and input buffering ability.

It should be noted that extremely good noise isolation at every stage of implementation is required for satisfactory operation of integrator circuits. Power supply rails must be stabilized with capacitors at points as close as possible to the op-amps, and it is recommended to use voltage regulators (such as LM7815 and LM7915) for powering the op-amps to isolate the circuit as much as possible from power line variations.

B. Circuit Design

We evaluate two separate approaches for double integration. In the first design, we propose a critically damped integrator structure consisting of two first order integrator stages interspaced with three high-pass filters that were used to remove DC and low frequency components in the signal before and after each integration stage. The second design is a replication of the best approach we have found in the literature, namely the underdamped double integrator of Viswanathan and Baghialakshmi [8]. We implement slight modifications to their original circuit design to improve its overall gain in order to be able to conduct a more fair comparison.

In both circuits, filters are constructed so that the transfer function of the circuit behaves as an integrator in the frequency range of interest, in this case 10 to 100 Hz. In the first circuit, first order high-pass and low-pass filters are cascaded in an interlacing pattern. A block diagram depicting the entire circuit and using the circuits given in Fig. 2 is shown in Fig. 3. The transfer function of each high-pass stage is given by

$$G_H(s) = \frac{-\frac{R_6}{R_5}s}{s + \frac{1}{R_5 C}} \tag{1}$$

From this equation we identify the cut-off frequency as $f_c = 1/(R_5 C)$ and the DC gain as zero. Conversely, the integrator,

or low-pass, stages each have a transfer function given by

$$G_L(s) = \frac{-\frac{1}{R_2 C}}{s + \frac{1}{R_1 C}} \tag{2}$$

Similarly, we note the cut-off frequency $f_c = 1/(R_1 C)$ and the DC gain $-R_1/R_2$. The instrumentation amplifier simply acts as a gain in this circuit, denoted as α. Each of the high-pass filters and each of the integrators have identical resistor and capacitor values. Therefore, the final transfer function can be represented as

$$\frac{V_{out}(s)}{V_{in}(s)} = \alpha G_H(s) G_L(s) G_H(s) G_L(s) G_H(s) \tag{3}$$

The circuit was cascaded such that the high-pass and integrator circuits interlace because the non-ideal behavior of the op-amps results in the integrator circuits developing a steady-state offset even with no input offset. This is due to leakage and bias currents around the op-amp building charge in the capacitor in the feedback path. Due to the high gains of the integrators, cascading them directly one after the other could result in the circuit becoming saturated simply as a result of these offsets. Looking at the idealized transfer function given in (3), we note that combining the two integrator transfer functions and three high-pass transfer functions yields

$$\frac{V_{out}(s)}{V_{in}(s)} = \alpha \left[\frac{-\left(\frac{R_6}{R_5}\right)^3 s^3}{\left(s + \frac{1}{R_5 C}\right)^3} \right] \left[\frac{\frac{1}{R_2^2 C^2}}{s^2 + \frac{2}{R_1 C} s + \frac{1}{R_1^2 C^2}} \right] \tag{4}$$

which indicates that the integration is due to a second order critically damped system. Also note that as $s \to \infty$,

$$G_L(s) G_L(s) \to \frac{1}{R_2^2 C^2} \frac{1}{s^2}$$

which means that for periodic input signals composed only of high frequencies, the steady-state output of the integrators will be very close to the true double integrated signal with a gain. The component values in the circuits shown in Fig. 2 were used for collecting data for the experimentally determined Bode plots. The resistors R_2 in the integrators were replaced by $22k\Omega$ resistors to increase the overall gain of the circuit for integrating the accelerometer signals.

In addition to the first circuit, we have replicated the double integration circuit built by Viswanathan and Baghialakshmi with some modifications [8]. In their original circuit, they used a second order integrator, thus performing the entire double integration process with a single op-amp. Their filter also allows the designer to choose a damping ratio. In [8] it was shown that true integration will start earlier for an underdamped system. In the modified circuit we built, the damping ratio was set to be $\zeta = 0.1$ ($\zeta < 0.3$ is recommended in [8]). We used the same instrumentation amplifier circuit as the input stage. The second order high-pass and integrator circuits are shown in Fig. 4, and a block diagram representing the structure of the entire circuit is shown in Fig. 5. As an addition to the original circuit given in [8], we inserted a second order high-pass filter before

(a) High-pass filter (b) Integrator

(c) Instrumentation amplifier
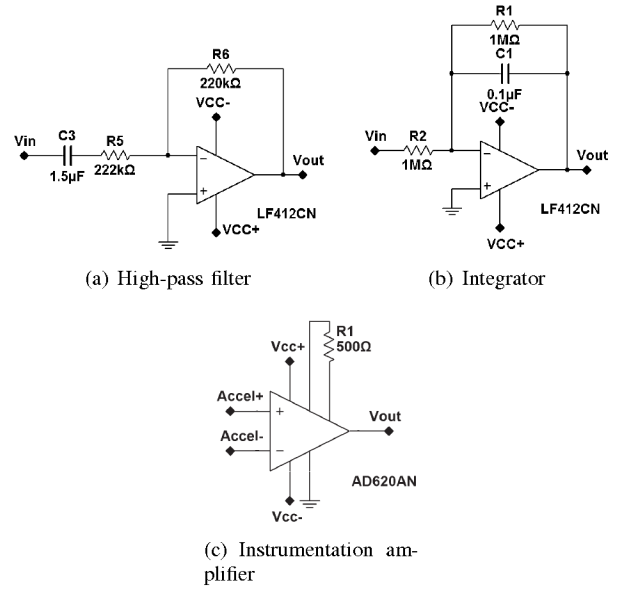
Fig. 2. Diagrams of the high-pass filter, the integrator, and the instrumentation amplifier used in our double integration circuit.
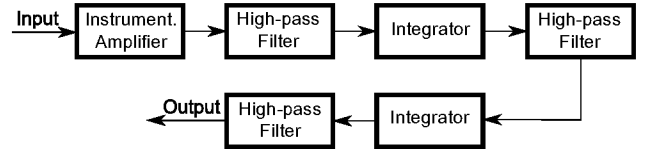
Fig. 3. A block diagram representing the signal path through our circuit.

the integrator to reduce DC offset. Also, after the double integrator, we inserted a first order low-pass filter with a gain of 100 and an inverting amplifier with a gain of 10 to reduce high frequency noise and increase the overall gain to a level comparable to the first circuit. For determination of experimental Bode plots, the low-pass filter and last inverting amplifier were removed to reduce the overall gain, in order to avoid saturation. Viswanathan and Baghialakshmi note that the transfer function of their integrator circuit is given by (5). This transfer function includes the simplifying assumptions that $C_2 = C$, $C_3 = C_4 = C/2$, $R_8 = R_9 = R$, and $R_{11} = R/2$. The transfer function for the second order high-pass filters used in our implementation of their circuit is given in (6). For the high-pass filter transfer function we have assumed that $C_1 = C_6 = C$.

$$G_{I2}(s) = \frac{R_{10}}{2R} \left[\frac{1}{1 + \frac{CR}{2} s \left[1 + \frac{CR_{10}}{4} s \right]} \right] \tag{5}$$

$$G_{H2}(s) = \frac{s^2}{s^2 + \frac{2}{R_4 C} s + \frac{1}{R_4 R_5 C^2}} \tag{6}$$

C. Determination of Bode Plots from Experimental Data

In order to verify that the circuit implementations were successful in replicating the theoretical behavior, we conducted a swept sine test on the circuits. For these experiments, we removed the AD620 instrumentation amplifiers, as

455
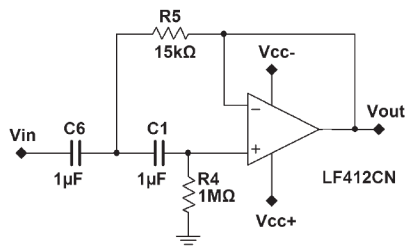
(a) Second order high-pass filter
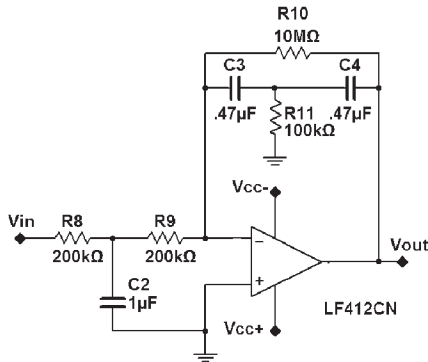
(b) Double Integrator

Fig. 4. Circuit diagrams of the second order high-pass filter and the double integrator used in our implementation of Viswanathan and Baghialakshmi's [8] circuit.
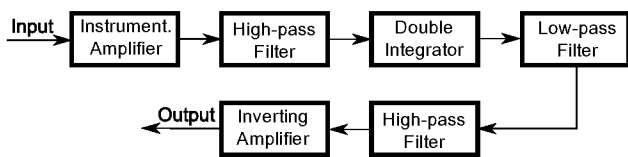
Fig. 5. A block diagram representing the signal path through our implementation of Viswanathan and Baghialakshmi's [8] circuit. The low-pass filter has a gain of -100, and the inverting amplifier has a gain of -10.

they only provide additional gain and impedance matching. In our circuit the resistors at the inputs of the integrators were switched to 1 MΩ in order for the entire circuit to have a gain less than one. In the second circuit, the gain was kept slightly higher since it is not as straightforward to reduce the gain of the integrator without altering the cut-off frequency and the damping ratio. Swept sine signals were generated by an Agilent 33120A 15 MHz function generator, and we recorded both the input signal to and output signal from the circuits at a sample rate of 1 kHz using a Quanser Q8 data acquisition board and QuaRC software. The amplitude of the swept sine input was 10 V peak-to-peak for our circuit, and 400 mV peak-to-peak for the second circuit, the difference being due to constraining output voltages between ±10 V to avoid saturation throughout the whole frequency sweep. The total duration of the signal was 180 seconds, and the frequency of the sine was logarithmicly swept from 0.1 Hz to 100 Hz. This range was wide enough to accurately capture the behavior of both circuits, because low frequency signal components (<10 Hz) are not integrated and high frequency
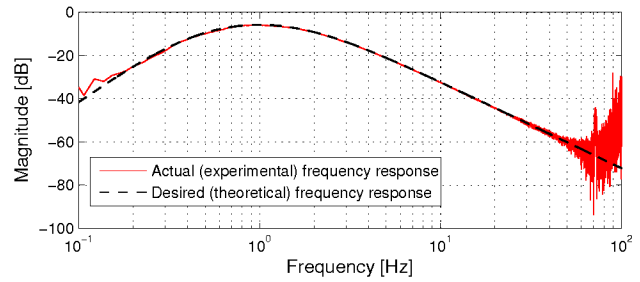
Fig. 6. The theoretical and experimentally determined Bode magnitude plots for our critically damped integrator circuit.
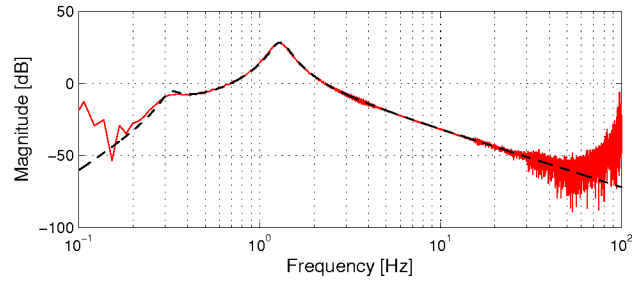
Fig. 7. The theoretical and experimentally determined Bode magnitude plots for the second circuit, with the underdamped double integrator of Viswanathan and Baghialakshmi.

components (>100 Hz) become lost at the noise floor. The MATLAB function `tfestimate` was used to compute an approximate overall transfer function for the circuit. These results are presented in the next section.

III. RESULTS & DISCUSSION

For our circuit, the theoretical and experimentally determined magnitude of the frequency responses match very well. Both the theoretical curve and the experimental estimate are plotted in Fig. 6. This good agreement indicates that we have a successful implementation of the theoretical behavior we desire. The three first-order high-pass filters have a combined slope of 60 dB/decade below the cut-off frequency, and the two integrators have a combined slope of -40 dB/decade. Similarly, the second circuit we implemented also well matches its theoretical behavior, as seen in Fig. 7. For both integration circuits, it is useful to note that there is approximately one decade of useful integration range before the signal becomes too small to distinguish from noise. This is in agreement with results reported by Ball and Lewis [4].

Another important test for these integrators is whether or not the time domain response is correct; i.e., whether they measure the position accurately based on only acceleration sensing. For this test, swept sine recordings of the speaker were taken from 1 Hz to 100 Hz, and the entire response for both circuits is shown in Figs. 8 and 9. Although the individual oscillations are not visible, an interesting observation can be made. Due to the underdamped integrator, high-pass filters and large gain at resonance, the circuit adapted from [8] does not accurately integrate the
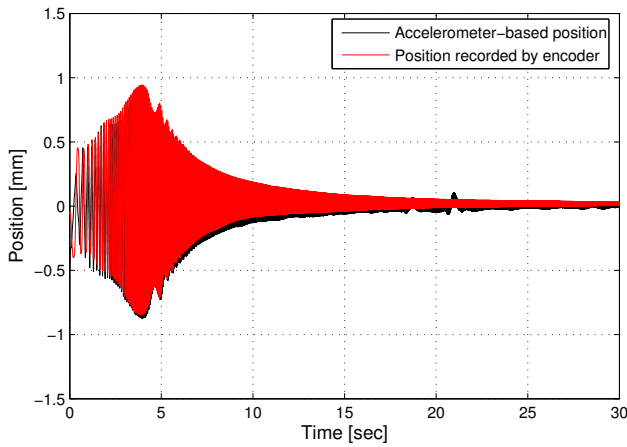
Fig. 8. The integrated position of the speaker compared to the linear encoder reading for a 30-second swept sine from 1 Hz to 100 Hz. Our critically damped integration circuit was used to process the accelerometer signal.
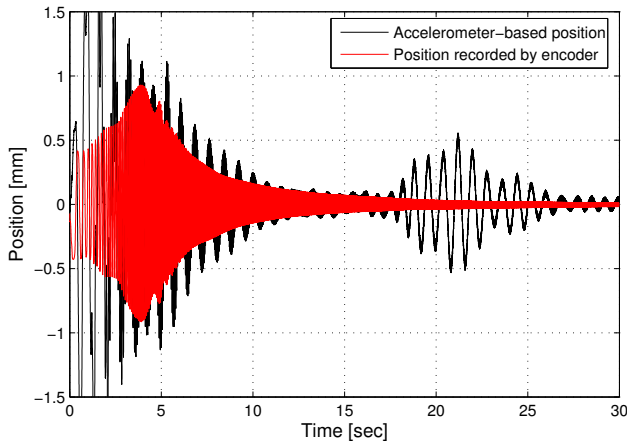
Fig. 9. The integrated position of the speaker compared to the linear encoder reading for a 30-second swept sine from 1 Hz to 100 Hz. The underdamped integration circuit adapted from [8] was used to process the accelerometer signal.

Fig. 10. The integrated speaker position compared with the linear encoder reading for a quasi-steady-state sawtooth input at 25 Hz. Our critically damped integration circuit was used to process the signal from the accelerometer.
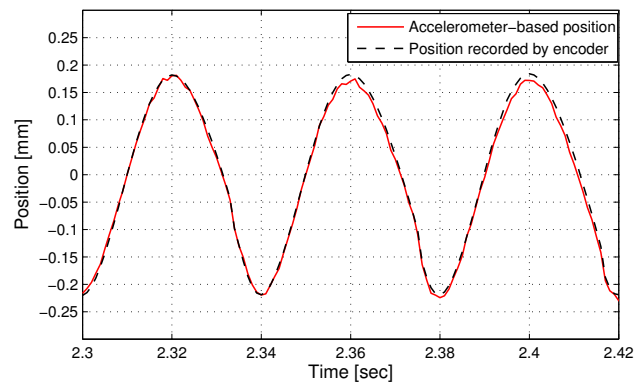
Fig. 11. The integrated speaker position compared with the linear encoder reading for a quasi-steady-state sawtooth input at 25 Hz. The underdamped integration circuit adapted from [8] was used to process the signal from the accelerometer.

swept sine signal (Fig. 9). Large oscillations are added to the small oscillations that represent the true motion of the speaker. The critically damped response of our circuit does not exhibit this undesirable behavior (Fig. 8). The oscillations at the beginning of the recording in Fig. 9 are due to the fact that the function generator was turned on at a low frequency before the swept sine was started, but the oscillations decay and then suddenly begin again due to noise or some other transient signal component about 16 seconds into the recording. The oscillations do not decay completely even by the end of the 30 second recording. This behavior is contrasted with a similar occurrence about 22 seconds into the recording using our critically damped integrator; the accelerometer based position does drift away from the mean briefly, but it quickly returns.

To show behavior during a quasi steady-state input, a sawtooth wave was played through the speaker at 25 Hz for 30 seconds and recorded. We give a close-up view of the response of each circuit in Figs. 10 and 11. At 25

Hz, it is clear that the circuit adapted from [8] is more accurate in terms of phase lag. Because the integrator is underdamped, the phase approaches $-180°$ faster than for a critically damped system. As a result, true integration begins earlier for the underdamped integrator than for the critically damped integrator.

The peaks of the accelerometer-based signal also appear to be clipped or noisy for the underdamped integrator circuit. This is a result of the fact that the signal-to-noise ratio is significantly worse for the underdamped circuit as a result of the integrator gain being lower. In order to keep the resonance peak from being so large as to saturate the circuit or cause instability, the overall gain of the circuit has to be lower. In addition, in order to achieve a low cut-off frequency in the integrator and a low damping ratio would require large capacitor and resistor values for the circuit design of the integrator. Considering that the feedback resistor is already 10 MΩ in the integrator for the second circuit, it would seem unwise to raise this value any higher.

However, it is clear that there is a trade-off between stability during transient inputs and steady-state accuracy. At higher frequencies, the responses of the circuits to steady-state inputs are nearly identical, because eventually the criti-

cally damped integrator has a nearly constant phase of $-180°$ and a magnitude slope of -40 dB/decade. This indicates that each circuit may be useful for different applications, but for frequency domain system identification it is clear that the critically damped response is preferable, because any transients or noise that do not reflect the behavior of the mechanical system decay quickly rather than "ring" inside the circuit for a long period of time.

Although we do not present explicit velocity data, we believe that our circuit is capable of accurately estimating velocity as well. Accurate position signals after double integration implies that accurate velocity signals exist after the first integrator stage. Hence our circuit can be used to obtain velocity measurements from accelerometers as well, as opposed to that of Viswanathan and Baghialakshmi, where double integration takes place in a single stage.

Despite the accurate position measurements from our circuit, it is still not reliable enough to use this position signal for closed-loop position control. The reason behind this lack of reliability is the fact that accelerations are measured with respect to the world coordinate, and any background vibration that can move the complete experimental setup will also be sensed, regardless of the speaker cone's movement with respect to the speaker base. A double accelerometer setup in which the second accelerometer will measure the speaker base position can be used to cancel out the effects of base vibration, and constitutes a direction for future work.

IV. Conclusion

We successfully measured position of vibrations generated by a speaker with an accelerometer by proper design and implementation of analog filter and integrator circuits. Long-term integration of acceleration for accurate estimations of velocity and position is only possible in continuous domain. Removal of DC offsets from signals before and after every stage of integration ensures accuracy and avoids drift and saturation. Position signals that can be measured with this method are limited to those that are lower-bounded in frequency. Nevertheless, our proposed integrator is well-suited for frequency domain system identification due to significant advantages it offers, such as minimal interference to system dynamics and ease of sensor attachment.

References

[1] H. A. Aldridge and J. N. Juang, "Experimental robot position sensor fault tolerance using accelerometers and joint torque sensors," *NASA Technical Memorandum 110335*, 1997.

[2] Y. K. Thong, M. S. Woolfson, J. A. Crowe, B. R. Hayes-Gill, and D. A. Jones, "Numerical double integration of acceleration measurements in noise," *Measurement*, vol. 36, no. 1, pp. 73–92, 2004.

[3] R. E. Mayagoitia, A. V. Nene, and P. H. Veltink, "Accelerometer and rate gyroscope measurement of kinematics: an inexpensive alternative to optical motion analysis systems," *Journal of Biomechanics*, vol. 35, no. 4, pp. 537–542, 2002.

[4] R. Ball and C. P. Lewis, "Effect of noise when deriving signals from accelerometers," *Measurement and Control*, vol. 15, pp. 59–61, 1982.

[5] M. Croker, "Determination of displacement by double integration of accelerometer signals," *Journal of Sound and Vibration*, vol. 93, no. 4, pp. 598–600, 1984.

[6] R. Balasubramanian, R. Howe, and Y. Matsuoka, "Task performance is prioritized over energy reduction," *IEEE Transactions on Biomedical Engineering*, vol. 56, no. 5, pp. 1310–1317, 2008.

[7] S. Harashima, "Vibration detecting device and vehicular road simulator employing the device," US Patent 5,540,099, 1996.

[8] R. Viswanathan and S. Baghialakshmi, "A direct acceleration and displacement meter using op-amps." *Indian J Tech*, vol. 12, pp. 536–539, 1974.

[9] C. P. Lewis and R. Ball, "An instrument for the measurement of structural vibrations," *The Journal of Strain Analysis for Engineering Design*, vol. 14, no. 4, pp. 165–169, 1979.